3D Point Cloud Based Spatio-Temporal Monitoring of Artificial and Natural Objects

Jens-André PAFFENHOLZ, Germany and Corinna HARMENING, Austria

Key words: Bridge surveying; Deformation measurement; Engineering survey; Laser scanning

SUMMARY

This paper aims to provide an overview of the field of 3D point cloud based spatio-temporal monitoring. The focus is on spatio-temporal monitoring of artificial and natural objects with the aid of 3D point clouds acquired by means of multi-sensor-systems (MSS) with a laser scanner as a main object capturing sensor.

First, we discuss the technical aspects of the MSS for 3D point cloud acquisition with respect to monitoring applications. In particular, the challenges and chances of the surface-based technique will be outlined. Second, we highlight some results of self-conducted experiments: We focus on the evaluation of an object's abstraction for epochal comparison by means of area-based and shape-based approaches as well as on loading tests of a historic masonry arch bridge. The first showcase deals with the abstraction of natural objects by means of B-spline surfaces. For this purpose, 3D point clouds of plant leaves are investigated with the aim to obtain measures of interest like overall sizes and area. For the second showcase, we present results of the load-induced arch displacements on a bridge by means of 3D point clouds acquired by terrestrial laser scanning. In detail, we discuss different approaches for the deformation analysis based on the captured 3D point clouds, i.e., the multiscale model-to-model cloud comparison (M3C2) algorithm or a parametric procedure by means of B-spline approximation. We conclude our paper with some perspectives on the upcoming work plan of the IAG working group 4.1.3 in close cooperation with the FIG commission 6 to make significant contributions to the 3D point cloud based spatio-temporal monitoring of artificial and natural objects. The next steps will be the abstraction of natural soil erosion scenes to quantify volumes. Our take home for the reader is: *we are open for your contributions and your participation in the working group and commission work*. The authors are happy to hear from you!

3D Point Cloud Based Spatio-Temporal Monitoring of Artificial and Natural Objects

Jens-André PAFFENHOLZ, Germany and Corinna HARMENING, Austria

MOTIVATION

This paper aims to pick up selected activities of the IAG working group (WG) 4.1.3 in the field of 3D point cloud based spatio-temporal monitoring of the period 2015 to 2019. In the past four years, the WG has focused on spatio-temporal monitoring of artificial and natural objects with the aid of 3D point clouds. Without loss of generality terrestrial laser scanners (TLS) are used to acquire the 3D point clouds. TLS has proven to be a suitable technique for spatio-temporal monitoring of artificial structures like bridges as well as of natural objects like plants, e. g., for phenotyping purposes. It allows the determination of object changes with high accuracy in the low millimeter level. In addition to a high spatial resolution, a high temporal resolution with up to 1 million points per second is possible. The main characteristic of the TLS is their surface-based data acquisition, resulting in a 3D point cloud with typically millions of 3D coordinates of individual points along with at least intensity information and optional color information.

In many monitoring applications, the TLS as the main object capturing sensor is embedded in a multi-sensor-system (MSS) for an efficient and effective data acquisition. Most likely, either the MSS or the object itself is in motion or in other words is characterized by a spatio-temporal behavior in terms of its location in 3D space. To consider the mandatory spatio-temporal behavior, usually referencing sensors with respect to a superior coordinate system and synchronization with respect to a proper time reference are used. It is noteworthy that there is no strict categorization for sensors to be either object capturing sensors or referencing ones. The TLS for example is a classical object-capturing sensor on the one hand. On the other hand, due to the high measurement frequency, it is possible to support, e.g., the referencing procedure of the MSS platform by making use of object information and knowledge about the environment, see e. g. (Bureick et al., 2019; Vogel et al, 2019).

The use of TLS in the scope of geodetic monitoring and geodetic deformation analysis in addition to the classical point-wise deformation analysis is a highly topical research field, e. g., (Wunderlich et al., 2016). There are solved questions and new challenges (Holst and Kuhlmann, 2016) which are mainly related to the surface-based data acquisition and the resulting high point density.

The outline of the paper is as follows: The Section 2 gives a brief overview of the several contributions in literature in the scope of monitoring with the aid of 3D point clouds acquired by TLS sensors. In Section 3, we will introduce basics about the approximation of 3D point clouds by means of B-spline surfaces. This section comes along with the first showcase dealing with the B-spline based approximation of plant leaves to quantify leaf areas. Section 4 introduces the second showcase presenting results of load-induced arch displacements on a bridge by means of 3D point clouds acquired by a TLS. Finally, Section 5 concludes the paper and provides a perspective to future work.

1. STATE OF THE ART

(Ohlmann-Lauber and Schäfer, 2011) propose an initial classification for analysis approaches for deformation modelling. The authors distinguish between methods utilizing the raw 3D point could (point- and point cloud-based strategies) and methods based on a modeled 3D point cloud (surface-, geometry- and parameter-based strategies) to obtain geometric object changes. One of the major challenges regarding the latter is the suitable modeling of the 3D point cloud to obtain object changes. (Neuner et al., 2016) give a detailed overview of modeling strategies for 3D point clouds.

In order to judge and interpret changes and differences in the context of a geodetic deformation analysis, the uncertainty budget of the sensor as well as the (geo-) referencing procedure and its uncertainty has to be taken into account. (Wujanz et al., 2017) propose an approach considering sensor uncertainties, in particular for the distance measurement. (Paffenholz, 2012) gives an overview of (geo-) referencing strategies as well as an efficient direct (geo-) referencing approach.

In the following, the spatio-temporal monitoring based on 3D point clouds is reviewed for selected applications mainly coming from the infrastructure-building sector, and, hence, with the focus lying on artificial measuring objects.

(Liebig et al., 2011) discuss a combined application for structural measurements and 3D point clouds acquired by means of TLS sensors with the aim to calibrate a numerical model for a highway bridge under different traffic conditions. In particular, 3D point clouds for a static load scenario as well as 2D profiles in driving direction under various speed scenarios are acquired. The authors report about the ability of a validation of their numerical model, here finite element model (FEM), with the 2D profiles of the TLS.

(Schill and Eichhorn, 2019) use 2D profiles of a TLS in order to monitor railway bridges. For two selected railway bridges, the authors demonstrate the benefits of applying the TLS technique to make use of the non-contact measurement technique with a high spatial and high temporal resolution. This allows for capturing temporally variable structural deformations more efficiently and in a much higher spatial resolution than typically used tactile sensors for the deformation monitoring of bridge structures.

(Truong-Hong and Lindenbergh, 2019) deal with deformation measurements of bridge structures due to increasing traffic load and aging structures by means of TLS. The authors introduce three approaches called point-to-surface (P2S), point-to-cell (P2C) and cell-to-cell (C2C) to measure the deformation of a structure using 3D point clouds. Furthermore, investigations about the impact of the selected reference surface or cell size to the achieved accuracy of deformation measurement are shown. As an example the authors present the task to measure the bridge's vertical clearance.

(Eling, 2009) reports about the structural monitoring of dams using a TLS sensor. The author splits his methodology into three parts (1) the deformation analysis and definition of a geodetic datum, (2) the 3D point cloud geo-referencing and (3) the analysis of the 3D point cloud using a voxel model and local filtering. The advantage is seen in a detailed spatial resolution of the structure, here a dam in Lower Saxony, Germany, and in the automation of the analysis.

(Holst et al., 2015) introduce an approach for the area-based deformation analysis of a radio telescope's main reflector using a TLS. The authors emphasize the need for an appropriate measurement concept and for pre-processing steps, e. g., data reduction, object segmentation and sensor calibration, when making use of TLS in applications for deformation analysis.

(Gojcic et al., 2019) focus on the challenge of point correspondences typically used in deformation analysis approaches, which do not expose the true 3D changes in non-deformed regions of the 3D point clouds. The authors propose an algorithm establishing point-wise correspondences in the feature space utilizing a neural network based approach, which is also able to handle outliers. Their proposed algorithm outperforms traditional approaches in terms of obtaining true 3D displacement vectors.

The approximation process of 3D point clouds describing a complex freeform shell by means of B-spline surfaces is the topic of (Schmitt et al., 2019). The authors point out the benefits of using 3D point clouds and their geometric approximation in the scope of the object's shape verification and its structural analysis. Furthermore, the interfacing between B-spline surfaces and FEM analysis is addressed.

In addition to the above-mentioned artificial objects, there are specific applications and questions addressing natural objects and their spatio-temporal monitoring by means of 3D point clouds. For instance, the research field plant phenotyping is noteworthy: (Dupuis et al., 2016) use 3D point clouds with regard to the growth analysis of plants. The authors point out the challenges stemming from natural objects with their typically irregular shapes and propose the approximation by means of B-spline surfaces.

(Landmann et al., 2019) report about realistic digital models of blue mussel dropper lines obtained from 3D point clouds. Centred on the 3D point clouds, a suitable descriptor for the mass distribution over the surface is identified and 3D printed surrogates of the blue mussel are developed for further testing. They are evaluated regarding their fit to the original 3D point cloud data of the live blue mussels.

A general overview about methodologies and approaches to yield differences of 3D point clouds with the focus on its implementation in standard software can be found, e.g., in (Holst et al., 2017).

2. METHODOLOGY FOR 3D POINT CLOUD APPROXIMATION

2.1 B-spline surfaces

Free-form curves and surfaces have been used as part of a standard approximation method for 3D point clouds in many engineering disciplines in the past decade. Examples for geodetic applications can be found in (Koch, 2009; Harmening and Neuner, 2015; Bureick et al., 2016) who model captured 3D point clouds by means of B-splines and non-uniform rational B-splines (NURBS). In addition, (Bureick et al., 2016; Xu et al., 2018) use B-splines for the monitoring of different structures, such as rails and arches. (Alkhatib et al., 2018) discuss a statistical evaluation of the B-spline-based approximation of 3D point clouds.

A B-spline surface of degree p and q is defined by:

$$\hat{\mathbf{S}}(u,v) = \sum_{i=0}^{n_\mathbf{P}} \sum_{j=0}^{m_\mathbf{P}} N_{i,p}(u) \cdot N_{j,q}(v) \cdot \mathbf{P}_{ij}$$

According to the previous equation, a surface point $\hat{\mathbf{S}}(u,v)$ is computed as the weighted average of the $(n_\mathbf{P}+1)\times(m_\mathbf{P}+1)$ control points $\mathbf{P}_{ij}$ (Piegl and Tiller, 1997, p. 100). The corresponding weights are defined by the functional values of the B-spline basis functions $N_{i,p}(u)$ and $N_{j,q}(v)$, which can be recursively computed (Cox, 1972; Boor, 1972). Two knot vectors, one in direction of the surface parameter u ($\mathbf{U} = [u_0, \dots, u_r]$) and one in direction of the surface parameter v ($\mathbf{V} = [v_0, \dots, v_s]$), split the B-spline's domain into knot spans.

Usually, only the location of the control points is estimated in a linear Gauß-Markov model when estimating a best-fitting B-spline surface. The choice of the optimal number of control points $(n_\mathbf{P}+1)$ and $(m_\mathbf{P}+1)$ to be estimated is a model selection problem and can be solved by classical model selection criteria or by structural risk minimization (Harmening and Neuner, 2016; Harmening and Neuner, 2017). In order to obtain a linear relationship between the observations and the unknown control points $\mathbf{P}_{ij}$, the B-spline's knots as well as its degrees are usually specified a priori. The use of cubic B-splines with $p = q = 3$ is a commonly accepted choice. The determination of the knots (known as knot adjustment problem) considerably affects the estimation of the B-spline surface. Therefore, in (Bureick et al., 2016; Bureick et al., 2019) different approaches based on Monte Carlo techniques and genetic algorithms are developed with regard to B-spline curves. Both approaches show an optimal selection of knots for curve approximation. Finally, convenient surface parameters u and v, locating the observations on the surface to be estimated, have to be a-priori allocated to the observations (Harmening and Neuner, 2016).

Hence, the workflow for the B-spline approximation of a 3D point cloud can be briefly summarized as follows: (1) pre-processing of the 3D point cloud, (2) model selection and parametrization, (3) knot vector adjustment and (4) estimation of the B-spline surface in a linear Gauß-Markov model.

2.2 Multiscale model-to-model cloud comparison

The multiscale model-to-model cloud comparison (M3C2) algorithm (Lague et al., 2013) establishes point-to-point correspondences for two 3D point clouds. At a first stage, the M3C2 algorithm neglects the full uncertainty budget of the 3D point clouds.

The starting point of the M3C2 algorithm is the calculation of core points in one of the 3D point clouds, i.e. called reference 3D point cloud. The core points can be all points of the reference 3D point cloud or an equally spaced, subsampled 3D point cloud. Thus, the core points are calculated as the mean of all points of the original 3D point cloud in a predefined radius.

Subsequently, for each core point the normal vector is calculated by means of a plane. This plane is estimated from points in a predefined radius. Along with the plane estimation, a variance is provided which indicates the local variation of the 3D point cloud. It is noteworthy, that no distinction is possible between a variation resulting from the surface roughness and the uncertainty of the laser scanner. This local variance can be seen as a precision.

Finally, the core points are projected along the normal vector into the reference 3D point cloud and the other 3D point cloud. The difference for both 3D point clouds is indicated by the distance of both projected points.

An implementation of the M3C2 algorithm is provided by the open source freeware Cloud Compare (www.cloudcompare.org). In addition to 3D point cloud to 3D point cloud differences, CloudCompare provides significant distance changes, the standard deviation of the core points from the plane estimation as well as the density of the core points at the projection scale.

3. APPLICATION OF THE METHODOLOGY TO SELECTED NATURAL AND ARTIFICIAL OBJECTS

3.1 Natural object: Characterization of plant leaves

Phenotyping, aiming to determine the external shape of a plant as well as changes due to growth or morphological adaptation, is becoming more and more important in plant breeding. The presented project deals with the spatio-temporal monitoring of cucumber plants with the objective of an automatic phenotyping in terms of the determination of leaf areas. The data basis of this project are time series of 3D point clouds, which are acquired by means of a robotic multi-sensor system as well as by means of a TLS (Paffenholz and Harmening 2014). In the first processing step, a spatial segmentation extracts the plant's individual leaves: Initially, a pre-segmentation is performed by means of an efficient graph-based bottom-up procedure. The result provides the basis for the second step, a statistically based region merging. Afterwards, the temporal relationships between the individual spatial segmentations are established by means of a shape-matching procedure based on dynamic time warping. During this step, corresponding segments acquired at different points in time are identified via their shape. Simultaneously, over-segmentations in the spatial segmentations are corrected, see Figure 1 for a final segmentation result. Further information can be found in (Paffenholz and Harmening 2014).

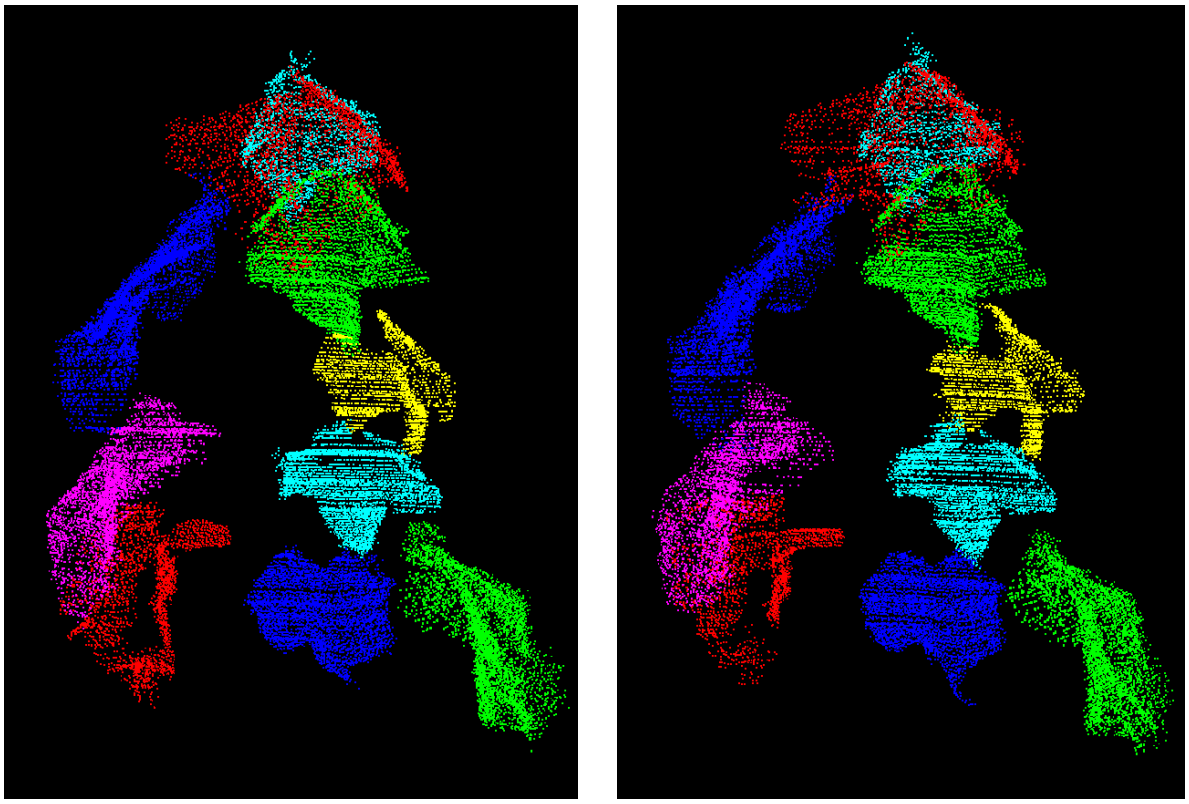

Figure 1: Temporal segmentation of two point clouds of the same plant. Points having the same colour belong to the same segment.

Afterwards, the segmented leaves are modelled by means of B-spline surfaces, providing the basis for the subsequent leaf area determination. Table 1 opposes the computed leaf areas A_B with values provided by a 3D digitizer, which is a standard, destructive working tool in plant phenotyping for determining leaf areas. By means of the manual, contact-based measuring system, thirteen characteristic leaf points are acquired, resulting into a generalized leaf model. It is known that these generalized models provide leaf areas that are about 10% too small. This behavior is clearly visible in Table 1: The B-spline based leaf area determination yields results, which are about 10 % larger than the areas provided by the digitizer in case of the leaves 3, 8, 10 and 17. For the remaining three leaves the results agree very well with the digitizer's results and, hence, are determined slightly too small as well. The reasons are incomplete acquisition of the respective leaf, cropping of boundary regions during the segmentation procedure as well as generalization of the boundary regions during the B-spline approximation. However, all leaf areas can be determined as well or even better than with the digitizer, indicating that the laborious and invasive procedure of manually digitizing the cucumber leaves can be replaced by the automatic procedure introduced in this project.

Table 1: Computed leaf areas A_B, acquired by means of a TLS as well as differences $\Delta A_{B,D}$ between the B-spline based leaf area determination and the digitizer results.

Leaf ID	A_B [cm^2]	$\Delta A_{B,D}$ [cm^2]	$\Delta A_{B,D}/A_B$

3	736.81	71.05	10.7 %
6	1094.20	27.66	2.6 %
8	1178.52	100.13	9.3 %
10	1529.59	151.03	11.0 %
13	1198.27	34.8	3.0 %
15	907.53	-18.48	-2 %
17	648.56	62.51	10.7 %

3.2 Artifical object: Loading tests on an historic railway arch bridge

The object under investigation in this case study is a historic masonry arch bridge over the river Aller near Verden (Lower Saxony, Germany). For details about the loading tests monitoring the reader is referred to (Paffenholz et al., 2018a; Paffenholz et al., 2018b; Wujanz et al., 2018a).

The 3D point cloud acquisition was carried out using a TLS of kind Zoller+Fröhlich (Z+F) IMAGER 5006 in periods of a constant load on the bridge. 3D point clouds for different load scenarios ranging from 1 MN up to 6 MN were captured and finally processed. The historic masonry arch bridge was made of circular brick arches of following dimensions: width $14\ m$, depth $8\ m$ and height $4 - 6\ m$.

Figure 2 shows the M3C2 differences for the load scenario of 5 MN in a 30-fold graduated color scale of ±15 mm. The maximum arch displacement here is 14 mm in the immediate vicinity of the threaded rods of the load application in the area of the apex of the arch. The decrease of the deformation in the direction of the pillars and in the East direction (upwards in Figure 2) to the unloaded area of the supporting structure is clearly visible.

For the approximation of the 3D point clouds by means of a B-spline surface, some preparatory steps were performed. Firstly, a buffering is realized, aiming to reduce the 3D point cloud in the margin areas and, hence, to handle data gaps in these areas, resulting into an improved B-spline approximation. Secondly, an initial approximation by means of a projection of the 3D point cloud on a regular grid is performed. This simple gridding approach is justified due to a homogenous curvature of the arch, which is characterized by non-occurring curvature changes. Sophisticated approaches to deal with complex surfaces, like Coons Patches, are discussed by (Harmening and Neuner, 2015).

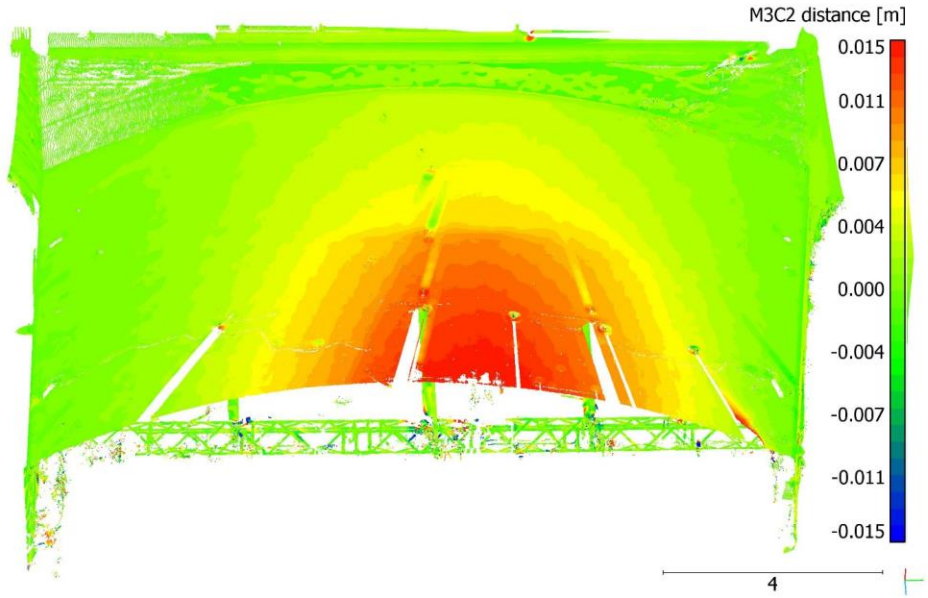

Figure 2: 3D point cloud to 3D point cloud differences (M3C2) for the load scenario of 5 MN. Clearly visible is an arch displacement of up to 14 mm (Paffenholz et al., 2018a).

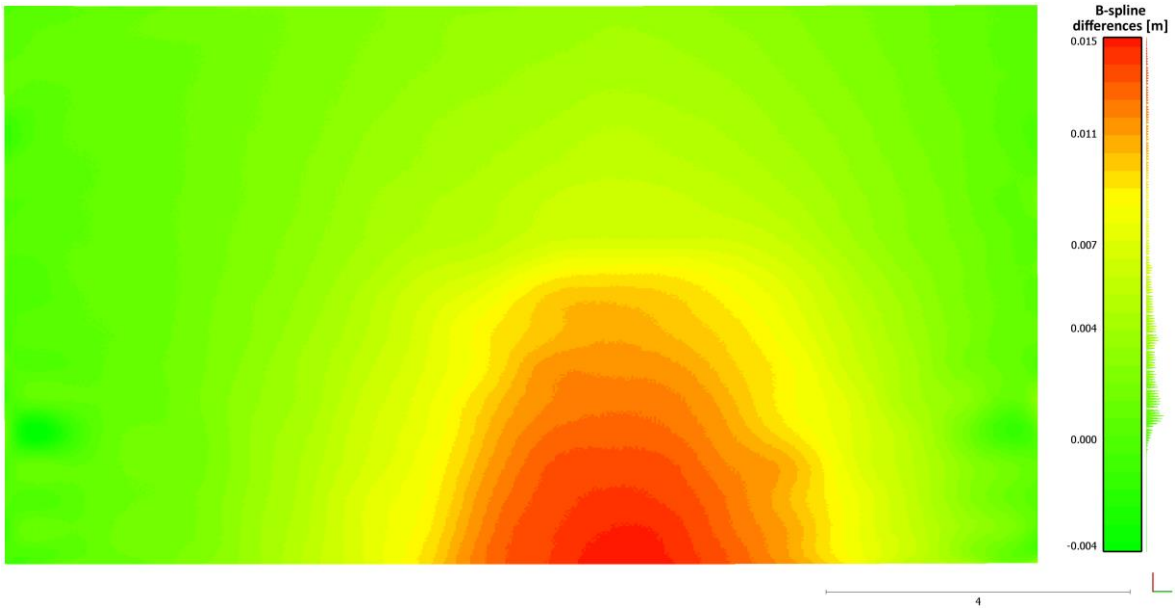

Figure 3: Exemplarily vertical deformation measures for the load scenario of 5 MN. The calculations were performed by means of difference for two B-spline surfaces of the unloaded epoch and the epoch with 5 MN load. Clearly visible is an arch displacement of up to 14 mm (Paffenholz et al., 2018a).

The grid size is chosen with respect to the dimensions of the 3D point cloud of the arch. Chosen is a size of 9 m, i.e., 400 grid cells, perpendicular to the bridge centerline and 14 m, i.e., 600 grid cells, in direction of the bridge centerline. This gridding results in nearly quadratic grid cells of size 0.022 m and each cell holds a sub 3D point cloud of up to ten 3D points of the entire 3D point cloud.

Based on the calculated B-spline surfaces, deformations of the individual epochs can be detected, exemplarily shown in Figure 3. Due to the fact that any point can be calculated for an estimated B-spline surface, the differences between two load scenarios can be easily determined. In this context, the points of the corresponding B-spline surface are calculated for each load scenario in a fixed grid of a given grid width. Thus, for each epoch, the function values of the B-spline surface are available in a grid that is uniform for all load scenarios.

When comparing the obtained deformation measurements by the M3C2 algorithm (Figure 2) and the B-spline approach (Figure 3), no considerable difference in the magnitude of vertical displacements can be found. As benefit of the B-spline approach over the M3C2 can be noted that a handling of data gaps due to occlusions in the 3D point clouds is possible. In addition, due to the parametrization of the 3D point cloud by mean of the B-spline approach the interdisciplinary data exchange is supported. Further results can also be found in (Paffenholz and Wujanz, 2019).

4. CONCLUSIONS AND OUTLOOK

This contribution aims to provide an overview of the 3D point cloud based spatio-temporal monitoring. The brief literature review states that this research field is quite new and still under development with solved questions and challenges to tackle. In particular the huge amount of indvidual 3D points in the cloud, their proper approximation and finally the statistical testing of differences in the scope of a deformation analysis are current research topics. For the statistical testing, the consideration of uncertainty information is mandatory. This can be seen as an independent research questions and is approached, e.g., by (Wujanz et al., 2018b).

In our ongoing research, we will move towards natural objects and their spatio-temporal behaviour. Recently, we evaluated the quantification of soil erosion of farmland in soil erosion monitoring areas in Lower Saxony, Germany, using 3D point clouds acquired by means of a TLS. The focus is on the approximation of 3D point clouds to yield the volume of soil erosions. For first results, see (Steinhoff-Knopp et al., 2019).

REFERENCES

Alkhatib, H., Kargoll, B., Bureick, J., Paffenholz, J.-A. (2018) Statistical evaluation of the B-splines approximation of 3D point clouds. In: Proceedings of the XXVI FIG International Congress -Embracing our smart world where the continents connect: enhancing the geospatial maturity of societies-, available via www.fig.net, Istanbul, Turkey.

Cox, M. G. (1972): The Numerical Evaluation of B -Splines. In: IMA J Appl Math 10 (2), S. 134–149. doi: 10.1093/imamat/10.2.134.

Boor, C. de (1972): On calculating with B-splines. In: Journal of Approximation Theory 6 (1), S. 50–62. doi: 10.1016/0021-9045(72)90080-9.

Bureick, J., Alkhatib, H., Neumann, I. (2019): Fast converging elitist genetic algorithm for knot adjustment in B-spline curve approximation. In: Journal of Applied Geodesy 13 (4), pp. 317–328. doi: 10.1515/jag-2018-0015.

Bureick, J., Vogel, S., Neumann, I., Unger, J., Alkhatib, H. (2019): Georeferencing of an Unmanned Aerial System by Means of an Iterated Extended Kalman Filter Using a 3D City Model. In: Photogrammetrie, Fernerkundung, Geoinformation 87 (5-6), S. 229–247. DOI: 10.1007/s41064-019-00084-x.

Bureick, J., Alkhatib, H., Neumann, I. (2016). Robust Spatial Approximation of Laser Scanner Point Clouds by Means of Free-form Curve Approaches in Deformation Analysis. In: Journal of Applied Geodesy, Vol. 10, No. 1, pp. 27–35, doi: 10.1515/jag-2015-0020.

Dupuis, J., Holst, C., Kuhlmann, H. (2016): Laser Scanning Based Growth Analysis of Plants as a New Challenge for Deformation Monitoring. In: Journal of Applied Geodesy 10 (1), S. 37–44. DOI: 10.1515/jag-2015-0028.

Eling, D. (2009). Terrestrisches Laserscanning für die Bauwerksüberwachung. PhD thesis. Munich : DGK (Reihe C, 641).

Gojcic, Z., Zhou, C., Wieser, A (2019): Robust pointwise correspondences for point cloud based deformation monitoring of natural scenes. In: Proceedings of the 4th Joint International Symposium on Deformation Monitoring (JISDM). Athens, Greece.

Harmening, C., Neuner, H. (2017). Choosing the optimal number of B-spline control points. Part 2: Approximation of surfaces and applications. In: Journal of Applied Geodesy, Vol. 11, No. 1, pp. 43–52, doi: 10.1515/jag-2016-0036.

Harmening, C., Neuner, H. (2016). Choosing the optimal number of B-spline control points. Part 1: Methodology and Approximation of Curves. In: Journal of Applied Geodesy, Vol. 10, No. 3, pp. 139–157, doi: 10.1515/jag-2016-0003.

Harmening, C., Neuner, H. (2015). A constraint-based parameterization technique for B-spline surfaces. In: Journal of Applied Geodesy, Vol. 9, No. 3, pp. 143–161, doi: 10.1515/jag-2015-0003.

Holst, C., Nothnagel, A., Blome, M., Becker, P., Eichborn, M., Kuhlmann, H. (2015). Improved area-based deformation analysis of a radio telescope's main reflector based on terrestrial laser scanning. In: Journal of Applied Geodesy, Vol. 9, No. 1, pp. 1–14, doi: 10.1515/jag-2014-0018 2015.

Holst, C., Kuhlmann, H. (2016): Challenges and Present Fields of Action at Laser Scanner Based Deformation Analyses. In: Journal of Applied Geodesy, Vol. 10, No. 1, pp. 17–25, doi: 10.1515/jag-2015-0025.

Holst, C., Schmitz, B., Schraven, A., Kuhlmann, H. (2017). Eignen sich in Standardsoftware implementierte Punktwolkenvergleiche zur flächenhaften Deformationsanalyse von Bauwerken? Eine Fallstudie anhand von Laserscans einer Holzplatte und einer Staumauer. In: zfv (Zeitschrift für Geodäsie, Geoinformation und Landmanagement), Vol. 142, No. 2, pp. 98–110, doi: 10.12902/zfv-0158-2017.

Koch, K. R. (2009).Fitting free-form surfaces to laserscan data by NURBS, In: allgemeine vermessungs-nachrichten (avn), Vol. 116, No. 4, pp. 134–140.

Lague, D., Brodu, N., Leroux, J. (2013). Accurate 3D comparison of complex topography with terrestrial laser scanner. Application to the Rangitikei canyon (N-Z). In: ISPRS Journal of Photogrammetry and Remote Sensing, Vol. 82, pp. 10–26, doi: 10.1016/j.isprsjprs.2013.04.009.

Landmann, J., Ongsiek, T., Goseberg, N., Heasman, K., Buck, B., Paffenholz, J.-A., and Hildebrandt, A. (2019). Physical modelling of blue mussel dropper lines for the development of surrogates and hydrodynamic coeffcients. Journal of Marine Science and Engineering, 7(3):65.

Liebig, J., Grünberg, J., Paffenholz, J.-A., Vennegeerts, H. (2011). Taktile und laserbasierte Messverfahren für die messtechnische Überwachung einer Autobahnbrücke. In: Bautechnik, Vol. 88, No. 11, pp. 749–756. doi: 10.1002/bate.201101514 2011.

Neuner, H., Holst, C., Kuhlmann, H. (2016). Overview on current modelling strategies of point clouds for deformation analysis. In: allgemeine vermessungs-nachrichten (avn), Vol. 123, No. 1-12, pp. 328–339.

Ohlmann-Lauber, J., Schäfer, T. (2011). Ansätze zur Ableitung von Deformationen aus TLS-Daten. In: Terrestrisches Laserscanning - TLS 2011 mit TLS-Challenge. DVW e.V. (eds.), 106. DVW-Seminar. Augsburg: Wißner-Verlag (Schriftenreihe des DVW, Band 66), pp. 147–157.

Paffenholz, J.-A. (2012). Direct geo-referencing of 3D point clouds with 3D positioning sensors. PhD thesis. Munich : DGK (Reihe C, 689), doi: 10.15488/4698.

Paffenholz, J.-A., Harmening, C. (2014): Spatiotemporal monitoring of natural objects in occluded scenes. In: Jan Schattenberg und Till-Fabian Minßen (Hg.): 4th International Conference on Machine Control & Guidance. Braunschweig, pp. 63–74.

Paffenholz, J.-A., Huge, J., Stenz, U. (2018a). Integration of Laser Tracking and Laser Scanning for Optimal Detection of Load Induced Arch Displacement. In: allgemeine vermessungs-nachrichten (avn), Vol. 125, No. 4, pp. 73-88.

Paffenholz, J.-A., Stenz, U., Neumann, I., Dikhoff, I., Riedel, B. (2018b). Belastungsversuche an einer Mauerwerksbrücke: Lasertracking und GBSAR zur Verformungsmessung. In: Mauerwerk-Kalender 2018. Jäger, W. (Eds.), Ernst & Sohn: Berlin, pp. 205-219, doi: 10.1002/9783433608050.ch9.

Paffenholz, J.-A., Wujanz, D. (2019). Spatio-temporal monitoring of a bridge based on 3d point clouds - a comparison among several deformation measurement approaches. In: Proceedings of the 4th Joint International Symposium on Deformation Monitoring (JISDM). Athens, Greece.

Piegl, L., Tiller, W. (1997): The NURBS Book. Second Edition. Berlin, Heidelberg: Springer (Monographs in Visual Communication). doi: 10.1007/978-3-642-59223-2.

Schill, F., Eichhorn, A. (2019). Deformation Monitoring of Railway Bridges with a Profile Laser Scanner. zfv (Zeitschrift für Geodäsie, Geoinformation und Landmanagement), Vol. 144, No. 2, pp. 109-118, doi: 10.12902/zfv-0248-2018.

Schmitt, C., Neuner, H.., Kromoser, B. (2019). Geodetic surface based methods for structural analysis during construction phase. In: Proceedings of the 4th Joint International Symposium on Deformation Monitoring (JISDM). Athens, Greece.

Steinhoff-Knopp, B., Eltner, A., Hake, F., Paffenholz, J.-A. (2019): Methoden zur skalenübergreifend hochaufgelösten Erfassung und Quantifizierung von Bodenerosion durch Wasser. In: Alkhatib, H. und Paffenholz, J.-A. (Hg.): Tagungsband GeoMonitoring 2019. Hannover, S. 75–89. doi: 10.15488/4514.

Truong-Hong, L., Lindenbergh, R. (2019): Measuring deformation of bridge structures using laser scanning data. In: Proceedings of the 4th Joint International Symposium on Deformation Monitoring (JISDM). Athens, Greece.

Vogel, S., Alkhatib, H., Bureick, J., Moftizadeh, R., Neumann, I. (2019): Georeferencing of Laser Scanner-Based Kinematic Multi-Sensor Systems in the Context of Iterated Extended Kalman Filters Using Geometrical Constraints. In: Sensors (Basel) 19 (10). DOI: 10.3390/s19102280.

Wujanz, D., Burger, M., Mettenleiter, M., Neitzel, F. (2017). An intensity-based stochastic model for terrestrial laser scanners. In: ISPRS Journal of Photogrammetry and Remote Sensing, Vol. 125, pp. 146-155, doi: 10.1016/j.isprsjprs.2016.12.006.

Wujanz, D., Burger, M., Tschirschwitz, F., Nietzschmann, T., Neitzel, F., Kersten, T. P. (2018b): Determination of Intensity-Based Stochastic Models for Terrestrial Laser Scanners Utilising 3D-Point Clouds. In: Sensors (Basel) 18 (7). DOI: 10.3390/s18072187.

Wujanz, D., Burger, M., Neitzel, F., Lichtenberger, R., Schill, F., Eichhorn, A., Stenz, U., Neumann, I., Paffenholz, J.-A. (2018a). Belastungsversuche an einer Mauerwerksbrücke: Terrestrisches Laserscanning zur Verformungsmessung. In: Mauerwerk-Kalender 2018. Jäger, W. (Eds.), Ernst & Sohn: Berlin, pp. 221-239, doi: 10.1002/9783433608050.ch10.

Wunderlich, T., Niemeier, W., Wujanz, D., Holst, C., Neitzel, F., Kuhlmann, H (2016). Areal deformation analysis from TLS point clouds – the challenge. In: allgemeine vermessungs-nachrichten (avn), Vol. 123, No. 11-12, pp. 340–351.

Xu, X., Kargoll, B., Bureick, J., Yang, H., Alkhatib, H., Neumann, I. (2018). TLS-based profile model analysis of major composite structures with robust B-spline method. In: Composite Structures, Vol. 184, pp. 814–820. doi: 10.1016/j.compstruct.2017.10.057.

BIOGRAPHICAL NOTES

Prof. Dr.-Ing. Jens-André Paffenholz received his diploma (Dipl.-Ing.) and his Ph.D. in Geodesy and Geoinformatics at the Leibniz University Hannover in 2006 and 2012, respectively. From 02-2014 to 11-2019, he has been postdoctoral fellow and the leader of the working group Terrestrial Laser Scanner Based Multi-Sensor Systems | Engineering Geodesy at the Geodetic Institute of the Leibniz University Hannover. Since 11-2019 he is a full professor for Geomatics for underground systems at Clausthal University of Technology. His research profile is based on laser scanning and multi-sensor systems with the aim of an efficient three-dimensional data acquisition for monitoring and change detection of natural and anthropogenic structures. He is active in national (DVW e. V. WG 4: "Engineering Surveys")

and international scientific associations (working group chair of IAG WG 4.1.3: "3D Point Cloud based Spatio-temporal Monitoring").

Corinna Harmening received her Master degree in Geodesy and Geoinformatics at the Leibniz Universität Hannover in 2013. Currently, she is a research assistant at the department for geodesy and geoinformation at TU Wien. She is active in international scientific associations (working group co-chair of IAG WG 4.1.3: "3D Point Cloud based Spatio-temporal Monitoring" and commission co-chair of FIG Commission 6: "Engineering Surveys").

CONTACTS

Prof. Dr.-Ing. Jens-André Paffenholz
Clausthal University of Technology
Department of Mine Surveying and Geoinformation – Professorship Geomatics
Erzstraße 18 – 38678 Clausthal-Zellerfeld, GERMANY
Email: jens-andre.paffenholz@tu-clausthal.de
Web site: www.igmc.tu-clausthal.de

Corinna Harmening, M. Sc,
TU Wien
Department of Geodesy and Geoinformation
Wiedner Hauptstr. 8/E120 – 1040 Vienna, AUSTRIA
Email: corinna.harmening@geo.tuwien.ac.at
Web site: www.geo.tuwien.ac.at